Deposition of Cadmium Sulfide Films by Decomposition of Thiourea in Basic Solutions

Peter C. Rieke* and Susan B. Bentjen

Materials Sciences Department, Pacific Northwest Laboratory, Richland, Washington 99352

Received August 7, 1992. Revised Manuscript Received October 6, 1992

Cadmium sulfide films were deposited on silicon wafer substrates by homogeneous decomposition of thiourea in basic solutions of amine complexed cadmium. The film morphology depended on the presence or absence of a cadmium hydroxide precipitate in solution and the presence or absence of a thin cadmium hydroxide film on the substrate. In the presence of the bulk precipitate, powdery poorly adherent films were formed; while in the absence of precipitate but with the cadmium hydroxide film, adherent, dense, specularly reflecting films were formed. In the absence of either bulk precipitate or substrate film, poor surface coverage was observed. X-ray photoelectron spectroscopy was used to detect the formation of the cadmium hydroxide film. Kinetic studies of the film growth demonstrated that film formation was essentially complete before the appearance of a bulk cadmium sulfide precipitate. After an initiation period, during which no discernable cadmium sulfide deposition occurred, the nucleation event occurred followed by crystal growth and no further nucleation of crystals. The behavior was very similar to the burst type nucleation found in homogeneous precipitation of powders. Analysis of the kinetic data supported decomposition of thiourea by the CdS film.

Introduction

Metal chalcogenide semiconductors are of interest in electronic and electrooptical applications especially for use in semiconductor lasers and infrared detectors and more recently as quantum dot structures.[1,2] Typically, cadmium, zinc, mercury, and/or lead are deposited as the sulfide, selenide, or telluride. The bandgap of these materials may be varied by preparing mixed compounds of varying ratios. Thin films can be deposited by sublimation, vacuum evaporation, and spray pyrolysis.[3]

Thin films of these materials may also be deposited from aqueous solution by the homogeneous precipitation method.[3-9] This method has many potential advantages over other thin-film fabrication techniques. As an aqueous solution method, it is relatively inexpensive and does not require complex equipment. Furthermore the stoichiometry is easily varied. One disadvantage is the lack of understanding of how nucleation and crystal growth can be controlled and how these processes influence film microstructure. The microstructure and properties of these films are highly dependent on the solution conditions used for deposition. The substrate may also influence the microstructure.

We have been interested in understanding how solution chemistry and the surface properties of substrates may be tailored to promote thin-film deposition from solution and control film microstructure.[10-14] The previous work on metal chalcogenide thin films[3-10] suggested these materials as suitable candidates for these studies as well as having important technical application. However, such studies are dependent on a detailed understanding of the composition of the solution and the species in solution that are actively involved in film deposition. We report in this paper our studies of cadmium sulfide thin-film deposition on silicon wafers. The films were deposited from basic cadmium solutions strongly complexed by amine. Sulfide was generated by homogeneous decomposition of thiourea. Cadmium sulfide was chosen as a prototypical metal chalcogenide, but these results should be qualitatively applicable to related semiconductor compounds.

Chopra and co-workers[3-6] and Kitaev and co-workers[7-9] have developed the basic method for deposition of metal chalcogenides by the homogeneous precipitation method. Thiourea or thioacetamide decomposes in basic solutions to form sulfide which, in the presence of complexed metals such as amine complexed cadmium, induces the precipitation of the metal sulfide. Thin films on substrates can be prepared by immersing the substrates in the precipitation solution. The thin films are not formed by simple absorption of colloidal particles from solution but are

(1) Henglein, A. *Chem. Rev.* **1989**, *89*, 1861.
(2) Steigerwald, M. L.; Brus, L. E. *Acc. Chem. Res.* **1990**, *23*, 183.
(3) Chopra, K. L.; Kainthla, R. C.; Pandya, D. K.; Thakoor, A. P. *Physics of Thin Films*; Academic Press: New York, 1982; Vol. 12.
(4) Sharma, N. C.; Kainthla, R. C.; Pandya, D. K.; Chopra, K. L. *Thin Solid Films* **1979**, *60*, 55.
(5) Kainthla, R. C.; Pandya, D. K.; Chopra, K. L. *J. Electrochem. Soc.* **1982**, *129*, 99.
(6) Kaur, I.; Pandya, D. K.; Chopra, K. L. *J. Electrochem. Soc.* **1980**, *127*, 943.
(7) Kitaev, G. A.; Uritskaya, A. A.; Mokrushin, S. G. *Russ. J. Phys. Chem.* **1965**, *39*, 1101.
(8) Kitaev, G. A.; Mokrushin, S. G.; Uritskaya, A. A. *Kollidnyi Zh.* **1965**, *27*, 51.
(9) Uritskaya, A. A.; Kitaev, G. A.; Mokrushin, S. G. *Kolloidnyi Zh.* **1965**, *27*, 767.
(10) Isshiki, M.; Endo, T.; Masumoto, K.; Usui, Y. *J. Electrochem. Soc.* **1990**, *237*, 2697.
(11) Tarasevich, B. J.; Rieke, P. C. *Materials Synthesis Utilizing Biological Processes*; Rieke, P. C., Calvert, P. D., Alper, M., Eds.; Materials Research Society: Pittsburg, PA, 1988; Vol. 174; pp 51.
(12) Tarasevich, B. J.; Rieke, P. C.; McVay, G. L. *The Bone-Biomaterial Interface*; University of Toronto Press: Toronoto, 1991.
(13) Bentjen, S. B.; Nelson, D. A.; Tarasevich, B. J.; Rieke, P. C. *J. Appl. Polym. Sci.*, in press.
(14) Tarasevich, B. J.; Rieke, P. C.; McVay, G. L.; Fryxell G. E.; Campbell, A. A. *Proceedings of the Conference on Ultrastructure Processing of Ceramics, Glasses, Composites, Ordered Polymers, and Advanced Optical Materials*; University of Florida, Gainesville, FL, 1991.
(15) Rieke, P. C.; Tarasevich, B. J.; Fryxell, G. E.; Bentjen, S. B.; Campbell, A. A. *Supramolecular Architecture in Two and Three Dimensions*; ACS Symp Ser. No. 499; Bein, T., Ed.; American Chemical Society: Washington, DC, 1992.

0897-4756/93/2805-0043$04.00/0

formed by heterogeneous nucleation and growth directly on the substrate. The term homogeneous precipitation is misleading. "Homogeneous" refers to the method of generating sulfide by reagent decomposition. This is as opposed to the "nonhomogenous" method of adding sulfide directly to solution as a salt.

Of major concern was the presence or absence of a cadmium hydroxide precipitate in solution. Kitaev et al.[7] and later Kaur et al.[6] have provided a thermodynamic equilibrium analysis of cadmium solutions complexed by amine. Kitaev et al.[7] suggested that the cadmium hydroxide precipitate was required for CdS film formation to occur; while Kaur et al.[6] found solution conditions under which CdS films were formed in the absence of $Cd(OH)_2$ precipitate. In these analyses only a limited number of equilibrium equations were considered. Specifically only formation of the $Cd(OH)_2$ precipitate, the $Cd(NH_3)_4^{2+}$ complex, and NH_3/NH_4^+ acid base equilibrium were considered. There are six cadmium amine complexes and six cadmium hydroxide complexes which may have a major influence on solution speciation. These authors identified, for various concentrations of added amine, pH values at which the solution was just saturated. However, these authors identified pH values above which $Cd(NH_3)_4^{2+}$ did not exist and below which this species did exist. In their analysis the presence or absence of $Cd(NH_3)_4^{2+}$ was considered important in evaluating the mechanism of film growth. It is not clear how this conclusion was reached. The definition of existence or nonexistence of $Cd(OH)_2$ precipitate is readily defined by the inequality IAP $\geq K_{sp}$, where IAP and K_{sp} are the ion activity product and the solubility product respectively for $Cd(OH)_2$. However, the complex formation equilibrium equations are a true equality relationship and $Cd(NH_3)_4^{2+}$ will exist under all conditions, albeit perhaps in small quantity. More importantly, other cadmium amine complexes will form and may dominate solution speciation.

In basic solution and in the presence of a variety of metals, including cadmium, thiourea decomposes to form the metal sulfide and cyanamide:[16-18]

$$Cd^{2+} + NH_2\text{–}CS\text{–}NH_2 + 2\ OH^- \rightarrow CdS + H_2CN_2 + 2\ H_2O$$

H_2CN_2 apparently only undergoes one dissociation to form HCN_2^- as we were able to find only a dissociation value reported for the first ionization.[19] The pK_a for this dissociation is 10.27, and for most of the results discussed below cyanamide does not dissociate. Kitaev et al.[20] reported the formation constant for $CdCN_2$ from CN^{2-} of 10^{-14} and obtained an X-ray powder diffraction pattern for this material. The possibility exists that $CdCN_2$ may form in the experiments described in this work.

Aqueous metal hydroxide species and colloidal metal hydroxide precipitates also catalyze the decomposition of thiourea to sulfide and cyanamide. Kitaev et al.[7] reported that $Cd(OH)_2$ precipitate catalyzes the thiourea decomposition. Norr[17] also demonstrated that PbS precipitates catalyze the decomposition of thiourea. Presumably, CdS may also be a good catalytic surface although this has not been specifically shown.

Shaw and Walker[21] have shown that, in the absence of catalytic metals or surfaces, thiourea decomposes in basic solutions to produce sulfide. These authors proposed formation of urea and subsequent decomposition of urea to ammonia and cyanate. They also suggested cyanamide as an intermediate prior to urea formation. These experiments were conducted in sealed ampoules at temperatures of 90–130 °C. Norr[17] has shown that, at room temperature, in 0.7 M sodium hydroxide and in the absence of a catalytic metal, thiourea does not produce appreciable quantities of sulfide detectable by precipitate formation upon addition of lead nitrate reagent.

In this work we have focused on the role of solution speciation in determining the CdS film composition and structure. Our approach has been to use equilibrium analysis of the cadmium, amine, and hydroxide system to predict the speciation in solution. The focus was on the formation of $Cd(OH)_2$ and $Cd(NH_3)_x^{2+}$ species as these species were previously found important in film formation. The formation of the hydroxide precipitate was confirmed experimentally. X-ray photoelectron spectroscopy was used to study the influence of solution composition on the substrate surface and on possible formation of a thin, $Cd(OH)_2$ film on the substrate. CdS film microstructure was determined with electron microscopy and XPS. We also report on a kinetic analysis of film growth.

Experimental Section

Cadmium nitrate, ammonium nitrate, and sodium hydroxide were obtained as reagent grade and used without further purification. Care was taken to prevent water and carbon dioxide adsorption in the solid sodium hydroxide. Thiourea was recrystallized once from hot methanol. CO_2-free water was prepared by boiling, under a nitrogen purge, 18×10^6 Ω water obtained from a reverse oosmosis/ion exchange water purification unit (Millipore). Stock solutions were 1.0 M $Cd(NO_3)_2$, 6.4 M NH_4NO_3, 0.5 M thiourea, and 6.0 M NaOH. These solutions were filtered under nitrogen with 0.1-μm filters (Millipore).

The substrates were cut from polished (100) silicon wafers (Silica-Source Technology Corp.) to a dimension of $^1/_2$ in. × 1 in. These samples were placed in wafer racks and treated briefly with a 0.1 M KOH solution followed by a 0.1 M HNO_3 solution and finally a water rinse. This procedure thickened the oxide layer from approximately 10 to 20 Å. The samples in racks were then transferred to the prepared cadmium amine solutions.

The deposition solutions were prepared from the stock solutions to be 0.1 M in $Cd(NO_3)_2$ and 1.0 M in NH_4NO_3. The pH was then adjusted with either the 6.0 M NaOH. The pH was measured with a combination electrode (Orion) calibrated against standard pH 7.00 and 10.01 buffers (VWR). The pH of the samples was also measured at the end of the precipitation. The pH varied by less than 0.1 pH unit from the initial pH. The solutions were prepared directly in 100 mL, clear, polycarbonate wide-mouth containers or in $^1/_2$-pint canning jars with an airtight lid. The jar lid was lined with parafilm to prevent contamination.

The substrates were emersed within 1 h of solution preparation. The freshly prepared thiourea solution was added as the last reagent, usually just before inserting the samples, but in some cases up to 3 days after inserting the samples. The solutions were stirred using $^1/_4$ in. × $^1/_{16}$ in. teflon stir bars and stirring plates set at the lowest possible stirring setting. The temperature was the ambient room temperature, about 25 °C. Samples were removed from the solutions at appropriate intervals, rinsed with water, ultrasonicated briefly with a low-power benchtop ultrasonicator until most of the visibly adhering particles were removed, and blown dry in a nitrogen stream.

(16) Bauer, R.; Wehling, I. *Z. Anal. Chem.* **1964**, *199*, 171.
(17) Norr, M. K. *J. Phys. Chem.* **1961**, *65*, 1278.
(18) Dvoinin, V. I.; Skornyakov, L. G.; Yatlova, L. E.; Degryarev, M. V.; Kitaev, G. A. *Z. Prikl. Khim.* **1982**, *55*, 213.
(19) Dean, J. A., Ed. *Lange's Handbook of Chemistry*; McGraw Hill: New York, 1985.
(20) Kitaev, G. A.; Bol'shchikova, T. P.; Yatlova, L. E. *Zh. Neorg. Khim.* **1971**, *16*, 3173.
(21) Shaw, W. H. R.; Walker, D. G. *J. Am. Chem. Soc.* **1956**, *478*, 5769.

Reagent grade sodium hydroxide and nitric acid were used to prepare solutions for titrations. National Bureau of Standards' primary standard grade potassium hydrogen phthalate was used to standardized the sodium hydroxide solution (4.97 M), and this was used to standardize the nitric acid solution (5.03 M). Titrations were done under flowing nitrogen to prevent CO_2 absorption in solution. Titrations were first performed from low pH to high pH, and the reverse titration was performed immediately to prevent loss of NH_3. Turbidity was determined qualitatively by visual observations of scattering of light from a 5-mW HeNe laser through a path length of approximately 3 cm. Changes from very turbid to clear solutions occurred over less than 0.5 pH units and distinct differences in turbidity could be observed over 0.1 pH units through this transition range. Such accuracy was sufficient for the purpose of this work.

Cadmium deposited on the films was determined by atomic adsorption analysis (Instrument Laboratories, IL-254 flame AA/AE). Standards were prepared by serial dilution of 1.0 ppt stock solution (0.1003 g of Cd metal in 10 mL of 50% HCl diluted to 100 mL). CdS was dissolved from silicon wafers of known area, approximately 0.75 cm^2, by shaking overnight in 10 mL of 5% aqueous nitric acid. These samples were used directly in analysis unless appropriate dilutions with 5% nitric acid solution were required.

Electron microscopy of the samples was performed on an Electroscan Environmental Microscope, Model E30, or on a JEOL JSM-U3 microscope. The samples were sputter coated with 100–200 Å of gold prior to analysis. Field emission micrographs were obtained on a Hitachi S-800 field emission SEM at 25 kV in the secondary electron emission mode. The samples were fractured and viewed at an oblique angle of 70–80° tilt from normal.

X-ray photoelectrron spectra were obtained on a Perkin-Elmer PHI 560 XPS/Auger/SIMS surface analysis system using a magnesium Kα photoline. The double-pass cylindrical mirror analyzer was calibrated to the 932.6 eV Cu 2p 3/2 and 75.14 eV Cu 3p 3/2 lines. Charge correction was calculated from difference of the observed carbon 1s binding energy to the 284.8-eV value for the carbon 1s binding energy. A Phillips APD 3620 X-ray powder diffraction unit was used to obtain powder diffraction data. A fixed Cu anode was used and operated at 40 kV and 25 mA. Scans were taken in step mode at 0.02°/s from 10 to 70° for 2θ. The phases were identified by comparison with the JCPDS/ICDD, powder diffraction data base, cd-rom version PDF-2, sets 1–40.

A solution speciation code, EQ3,[22,23] was used to solve the equilibrium equations interatively and to output the concentration of each solution species listed in Table I as well as the saturation with respect to the CdS and $Cd(OH)_2$ precipitates. While the equilibrium values have been written in the conventional manner, the actual reactions were modeled using Cd^{2+}, NH_3, NO_3^-, S^{2-}, and H^+ as the primary species from which all others were formed. The input for mass balance assumed that solutions were prepared from NH_4NO_3, $Cd(NO_3)_2$, and Na_2S while the pH was adjusted with NaOH. This was as close to the actual experimental conditions as could be obtained. The primary difference was that thiourea was used to slowly and homogeneously generate sulfide ion and was not added as a salt. The actual formation of solid phases was not modeled, and only supersaturations with respect to a given solid were calculated. Thus, the results modeled the initial solution conditions before precipitation occurred. No attempt was made to model the progress of the precipitations as this would have required unrealistic assumptions about the kinetics of solid-phase precipitations and thiourea decomposition.

Results and Discussion

A series of CdS films were formed by varing solution pH and time of deposition. Solutions 0.1 M in total $Cd(NO_3)_2$ and 1.0 M NH_4NO_3 were adjusted to the desired pH by addition of base. The silicon wafer substrates were inserted and an aliquot of thiourea added. Thiourea decomposed to produce sulfide that precipitated with cadmium to form the highly insoluble CdS ($\log K_{CdS} = -26.1$; see Table I). Substrates were removed from solution at various times up to 6 days, and the CdS films characterized by various methods. A CdS precipitate also formed in bulk solution. The onset of bulk precipitation depleted the solution of reagents, and the experiment was terminated at this point.

Table I. Cumulative Formation and Solubility Constants for the Cd^{2+}, NH_3, OH^-, S^{2-} System

rxn	stochiometric reaction	equilibrium const
1	$NH_4^+ \leftrightarrow NH_3 + H^+$	$pK_a = 9.24$
2	$Cd^{2+} + OH^- \leftrightarrow Cd(OH)^+$	$\log K_{11} = 3.92$
3	$Cd^{2+} + 2(OH^-) \leftrightarrow Cd(OH)_2$	$\log K_{12} = 7.65$
4	$Cd^{2+} + 3(OH^-) \leftrightarrow Cd(OH)_3^-$	$\log K_{13} = 8.70$
5	$Cd^{2+} + 4(OH^-) \leftrightarrow Cd(OH)_4^{2-}$	$\log K_{14} = 8.65$
6	$2Cd^{2+} + (OH^-) \leftrightarrow Cd_2(OH)^{3+}$	$\log K_{21} = 4.61$
7	$4Cd^{2+} + 4(OH^-) \leftrightarrow Cd_4(OH)_4^{4+}$	$\log K_{44} = 23.15$
8	$Cd^{2+} + NH_3 \leftrightarrow Cd(NH_3)^{2+}$	$\log K_{N1} = 2.65$
9	$Cd^{2+} + 2NH_3 \leftrightarrow Cd(NH_3)_2^{2+}$	$\log K_{N2} = 4.75$
10	$Cd^{2+} + 3NH_3 \leftrightarrow Cd(NH_3)_3^{2+}$	$\log K_{N3} = 6.19$
11	$Cd^{2+} + 4NH_3 \leftrightarrow Cd(NH_3)_4^{2+}$	$\log K_{N4} = 7.12$
12	$Cd^{2+} + 5NH_3 \leftrightarrow Cd(NH_3)_5^{2+}$	$\log K_{N5} = 6.80$
13	$Cd^{2+} + 6NH_3 \leftrightarrow Cd(NH_3)_6^{2+}$	$\log K_{N6} = 5.14$
14	$H_2S \leftrightarrow HS^- + H^+$	$pK_{S1} = 6.97$
15	$HS^- \leftrightarrow S^{-2} + H^+$	$pK_{S2} = 12.9$
16	$H_2O \leftrightarrow H^+ + OH^-$	$\log K_w = -14.0$
17	$Cd^{2+} + 2(OH^-) \leftrightarrow Cd(OH)_2(s)$	$\log K_{Cd(OH)_2} = -13.65$
18	$Cd^{2+} + S^{2-} \leftrightarrow CdS(s)$	$\log K_{CdS} = -26.1$
19	$H_2CN_2 = HCN_2^- + H^+$	$pK_{C1} = 10.27$
20	$HCN_2 = CN_2^{2-} + H^+$	pK_{C2} = unknown
21	$Cd^{2+} + CN_2^{2-} = CdCN_2$	$\log K_{CdCN_2} = -14.0$

The amine and hydroxide complexes of cadmium are formed in the solutions.[19,24] At constant total cadmium and amine concentrations, pH was the variable that controlled solution speciation. Cadmium is strongly complexed by amine to form $Cd(NH_3)_x^{2+}$ species. The cumulative formation constants for x up to 6 are listed in Table I. The primary influence of pH on cadmium complexation is to determine the NH_3/NH_4^+ ratio and hence the free amine available for cadmium complexation. The pH range of interest in film formation ranged from 7.0 to 11.0, and as the pK_a for ammonium dissociation is 9.24, pH had a strong influence on availability of amine for cadmium complexation.

Cadmium forms a variety of complexes with hydroxide (see Table I), and in moderately basic solutions a $Cd(OH)_2$ precipitate will form. The presence or absence of this precipitate was considered by Kitaev et al.[7] and Kaur et al.[6] to be particularly important in the formation of high-quality films. Because of the influence of pH on amine concentration and hence on free cadmium concentration, the cadmium hydroxide speciation and conditions for precipitation were not simply dependent on pH. In addition, the formation of a precipitate is often dependent on kinetic factors influencing formation and dissolution of the precipitate. Thus, theoretical prediction of supersaturation and experimental observation of $Cd(OH)_2$ precipitation were compared.

As documented in Table I, the number of equilibrium species associated with the system of interest in this study is quite large and complex. The full equations describing solution speciation were modeled using the EQ3 solution speciation code.

(22) Jenne, A., Ed., *Chemical Modeling in Aqueous Systems*; ACS Symp. Ser. No. 93; American Chemical Society: Washington, DC, 1979.

(23) Wolery, T. J. *EQ3NR: A Computer Program for Geochemical Aqueous Speciation-Solubility Calculations*; Lawrence Livermore Laboratory, 1983. Available from National Technical Information Service 5285 Port Royal Rd., Springfield, VA, 22161.

(24) Baes, C. F.; Mesmer, R. E. *The Hydrolysis of Cations*; Wiley: New York, 1976.

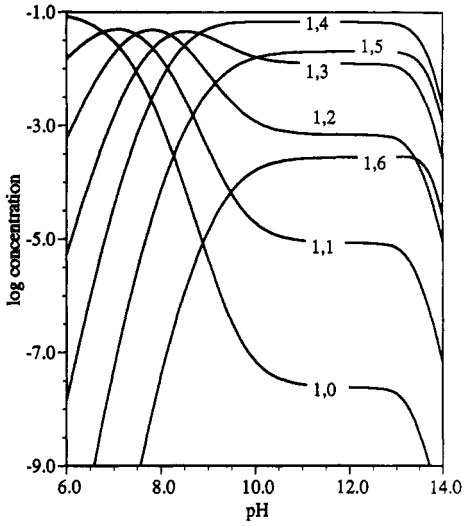

Figure 1. Calculated $Cd(NH3)_x^{2+}$ speciation curves versus pH for 0.1 M total $Cd(NO_3)_2$ and 1.0 M total NH_4NO_3. Species are denoted (1,x) where x is the number of complexing amine groups.

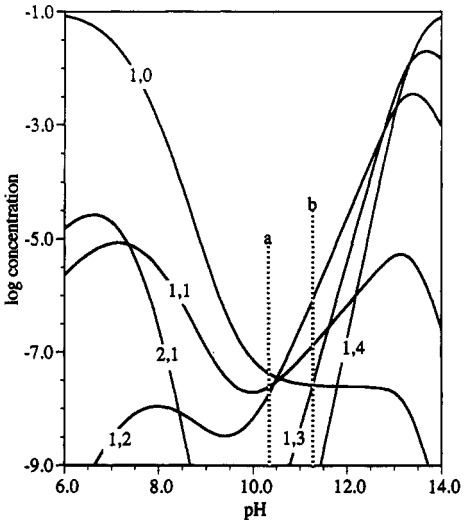

Figure 2. Calculated $Cd_x(OH)_y^{2x-y+}$ speciation curves versus pH for 0.1 M total $Cd(NO_3)_2$ and 1.0 M total NH_4NO_3. Species are denoted (x,y) where x and y denote the stoichiometry. Also marked with dashed lines are the observed (a) and calculated (b) values of pH above which $Cd(OH)_2$ precipitated.

Figure 1 presents the speciation for the amine complexed species, $Cd(NH_3)_x^{2+}$, where x ranges in integer values from 0 to 6. Each species is denoted in the figure by a notation of the form 1,x. No species containing more than one cadmium atom are formed. In the pH range of primary interest, 7.0–11.0, the major species changes from $Cd(NH_3)^{2+}$ at pH 7.0 to $Cd(NH_3)_4^{2+}$ above pH 9.0. The species $Cd(NH_3)_5^{2+}$ and $Cd(NH_3)_3^{2+}$ are also in significant concentration above pH 9.0. Above this pH the speciation shows little variation except at very high pH were $Cd_x(OH)_y^{2x-y+}$ species become important. Note that the free cadmium concentration falls rapidly from 0.1 M to nanomolar concentrations in the 6.0 to 10.0 pH range.

Presented in Figure 2 are the concentrations of the $Cd_x(OH)_y^{2x-y+}$ species versus pH. Each species denoted by x,y. In this case x can be 1, 2, or 4. However, at this total cadmium concentration the species $Cd_4(OH_4)^{4+}$ is negligible and is not shown in the figure. Also marked in the figure are the pH value, 11.3, at which the solution was calculated to be just saturated with respect to $Cd(OH)_2$ and the pH value, 10.4, above which the hydroxide

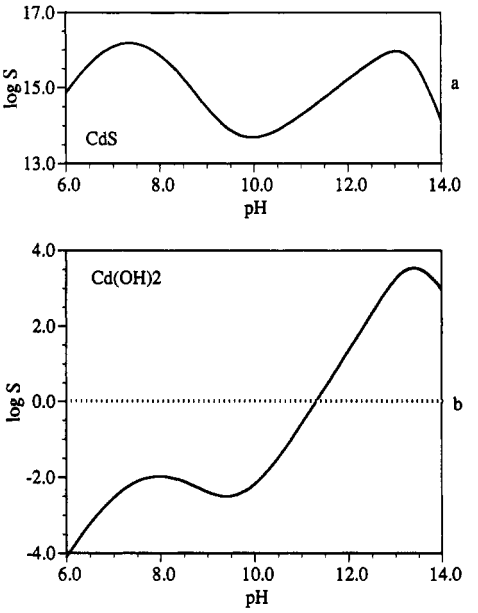

Figure 3. Calculated supersaturation curves expressed as log S versus pH for CdS (a) and $Cd(OH)_2$ (b).

precipitate was observed to form. This is explained in greater detail below.

At low pH the major species is free cadmium (1,0). As pH increases, the free cadmium concentration falls rapidly to less than micromolar concentrations, but it is still the major species, excluding amine species, until the pH reaches 10.5. Above this pH the species $Cd(OH)_2(aq)$ and increasingly $Cd(OH)_3^-$ and $Cd(OH)_4^{2-}$ dominate the speciation. The decrease in total concentration of hydroxide species in the middle pH ranges reflects the effect of amine complexation shown in Figure 1.

Parts a and b of Figure 3 plot the supersaturation ratio for the CdS and $Cd(OH)_2$ precipitates, respectively. The numerical values are the logarithm of the supersaturation ratio, S, where $\log S = \log (IAP/K_{sp})$ and IAP is the ion activity product and K_{sp} the solubility constant for the particular precipitate. For CdS it was assumed that all thiourea decomposed to sulfide and was equilibrated with HS^- and H_2S. Regardless of pH, the solutions are very supersaturated by a factor of about 10^{15}. While this should be regarded as a maximum possible value, it does demonstrate that very little thiourea decomposition must occur before supersaturation is achieved. For example, at pH 9.5 the free cadmium concentration is $10^{-6.5}$ M, and since the K_{sp} is $10^{-26.1}$, the sulfide concentration must exceed $10^{-19.6}$ M. The ratio of HS^-/S^{-2} ratio is 10^4 at this pH and thus the amount of decomposed thiourea must exceed the negligible value of $10^{-15.6}$ M to reach supersaturation. $Cd(OH)_2$ is undersaturated below pH 11.3 and supersaturated above this value. However, for the pH region 7.0–9.8 the undersaturation varies little with pH. Above pH 9.8 the saturation increases rapidly with pH.

Kitaev et al.[7] and Kaur et al.[6] have presented thermodynamic analyses of this same solution system but considered only reactions 1, 11, 16, and 17 of Table I. These authors predicted supersaturation with respect to $Cd(OH)_2$ at pH 11.2 in good agreement with our value of 11.3. However, these authors predicted $Cd(NH_3)_4^{2+}$ did not exist above pH 11.5 but did exist below this pH value. Contrary to this conclusion and as shown in Figure 1, the vast majority of cadmium is complexed as one of the amine species at any pH above 7.0 and specifically as the

$Cd(NH_3)_4^{2+}$ species at pH above 8.8. In the region where $Cd(NH_3)_4^{2+}$ dominates, the species $Cd(NH_3)_3^{2+}$ and $Cd(NH_3)_5^{2+}$ also make a significant contribution to the complexation of cadmium. Only above pH 13.5 does the concentration of $Cd(OH)_4^{2-}$ exceed that of $Cd(NH_3)_4^{2+}$.

As noted above, in basic solution and in the presence of a variety of metals, aqueous metal hydroxide species, metal hydroxide precipitates, and metal sulfide precipitates, thiourea decomposes to form the metal sulfide and cyanamide.[16-18] The times observed, in this work, for first formation of a bulk precipitate were used qualitatively to assess the relative rates of thiourea decomposition. Our observations are consistant with literature reports. At pH 7.0 decomposition was negligibly slow in the absence of any $Cd(OH)_2$, and experiments were terminated after 6 days without significant amounts of bulk precipitate forming. The decomposition rate increased with increased pH. At pH 9.5 complete precipitation occurred in about 60 h. At pH 10.5, where a small quantity of $Cd(OH)_2$ precipitate was present, CdS precipitation was complete in 1–2 h. At pH above 11.0, where substantial amounts of $Cd(OH)_2$ precipitate was present, the yellow CdS precipitate appeared in a few minutes. The presence of a $Cd(OH)_2$ precipitate greatly enhanced thiourea decomposition kinetics compared with decomposition in solutions of slightly lower pH in which the precipitate was not formed.

Powder X-ray diffraction patterns were obtained for the bulk precipitate formed in the film deposition solutions. The major phase in most samples was β-CdS (Hawleyite), but many samples also contained a minor phase of α-CdS (Greenockite). The phases were identified by observing the three peaks of α-CdS centered at 2θ value of 26.2 and the single peak of β-CdS at the same location. In some cases these peaks were neither a triplet nor a sharp singlet but a broad peak, suggesting a poorly crystalline material.

$CdCN_2$ was occasionally found as a minor phase. Using recrsytallized thiourea helped reduce the amount of $CdCN_2$ formed but did not completely eliminate this phase. For most of experiments 0.25 M thiourea was used; however, in a few samples the solution contained 0.5 M thiourea—a 5-fold excess of thiourea over total cadmium concentration. Unexpectedly, the use of excess thiourea favored formation of $CdCN_2$.

Crystalline $Cd(OH)_2$ was not present except in a very small quantity in one sample. This was somewhat surprising since many of the samples, especially those at high supersaturation with respect to $Cd(OH)_2$, formed a white gellike precipitate shortly after solution preparation. In addition, we observed that the $Cd(OH)_2$ gel transformed to a crystalline phase over a period of a few hours in the absence of thiourea. Oswald and Asper[25] report that β-$Cd(OH)_2$ is prepared by aging of basic amine complexed cadmium solutions. Apparently, the sulfide that formed from thiourea decomposition easily displaced the hydroxide to form CdS.

Titrations of a 0.1 M $Cd(NO_3)_2$ and 1.0 M NH_4NO_3 solution were used to determine the pH at which $Cd(OH)_2$ precipitation, and dissolution occurred. Thiourea was not added in this instance. The initial pH of the solutions was less than 5.0 due to the dissociation of NH_4^+, and complexation of cadmium to provide a slight acidity. Base was added to an appropriate end pH, and then acid added to reverse the titration. The turbidity of the solutions were monitored visually using a HeNe laser. By use of a laser the appearance or disappearance of a solid phase could be much more accurately determined by visual inspection dependent upon scattering of room light. As expected, no significant scattering of light occurred regardless of pH for the titration in the absence of cadmium.

On the forward titration of the solution containing cadmium, a HeNe visible precipitate became apparent at pH 10.4. At pH 10.6 the solution rapidly became very turbid with a heavy gelatinous precipitate. On reverse titration, the precipitate remained present until the pH reached 10.0, at which point the solution cleared rapidly. These values were significantly below the 11.3 value predicted in Figure 3b for the supersaturation of $Cd(OH)_2$. We do not take this discrepancy to suggest an error in calculated value but that the method of solution preparation resulted in metastable precipitate formation. At pH values from about 9.5 to 10.4, addition of 5 M NaOH resulted in localized high pH and formation of small quantities of a precipitate that dissolved upon stirring. As the pH approached 10.4, the amount of precipitate increased and became more persistent. Clearly, the kinetics of dissolution became slow with increasing pH and the observed value of 10.4 for formation of a permanent precipitate under estimated the true value. The occurrence of a localized precipitate in the pH 9.5–10.4 range correlates well with the point in Figure 3b where the value of log S for $Cd(OH)_2$ begins to increase rapidly with pH. In this region a small localized increase in pH results in a large increase in localized supersaturation and formation of greater quantities of precipitate. Below this region, variation in pH had little effect on log S. Thus, practically speaking, it was difficult to prepare a solution above 10.4 without some presistent precipitate formation due to the slow kinetics of dissolution near the equilibrium saturation value.

These titrations followed closely the behavior observed in film growth solutions except that, if solid sodium hydroxide was used in solution preparation, the precipitate initially formed at a lower pH and persisted to a lower pH value upon addition of acid. Localized precipitate formation was less pronounced with the 6 M NaOH used to prepare most of the solutions but did not eliminate this effect. Since, as shown below, the presence or absence of $Cd(OH)_2$ precipitate is of major concern in film formation, the important pH value in this regard is the 10.4 value observed in experiments. Practically, a pH lower by 0.2–0.3 units was needed to ensure that no $Cd(OH)_2$ precipitate formed.

Shown in Figure 4 are scanning electron micrographs of CdS films deposited at various values of pH. The experiments were terminated shortly after formation of the bulk precipitate and the samples were removed from solution. Adhered particles of bulk precipitate could be removed by ultrasonication in distilled water. Some adhered particles remained and these can be identified as the scattered spherical particles that appear white in the photographs because of charging. Films on samples removed just before the bulk precipitate began to form in significant quantities were very similar to those shown in the Figure 4, except that few adhered particles were observed. This is discussed in more detail under the results

(25) Oswald, H. R.; Asper, R. *Preparation and Crystal Growth of Materials with Layered Structures*; Lieth, R. M. A., Ed.; D. Reidel: Dordrecht, Holland, 1977.

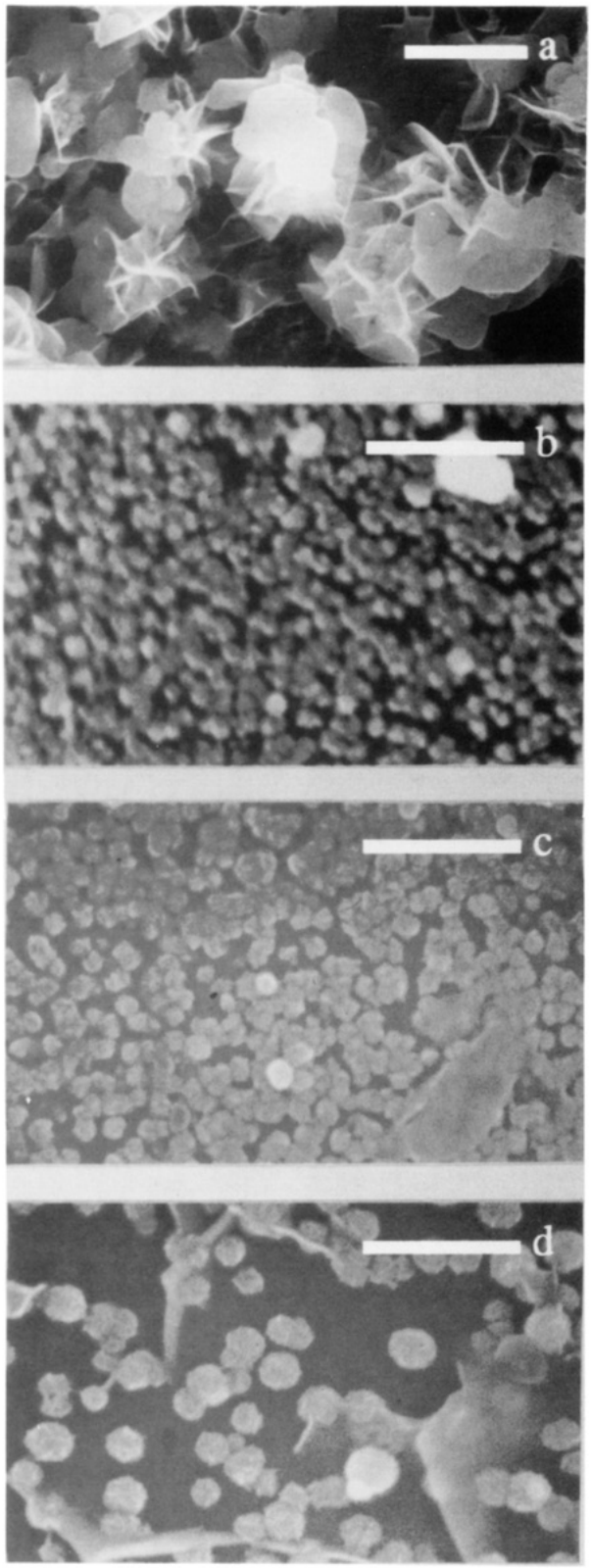

Figure 4. Scanning electron micrographs of CdS films deposited at various solution pH values of 10.54 (a), 10.03 (b), 9.63 (c), and 8.97 (d). The scale bar in (a) represents 5 μm, while the scale bars in (b)–(d) represent 1 μm.

on rates of film formation.

Two distinct morphologies can be identified from the micrographs. The sample obtained at a pH of 10.54 (Figure 4a) had a complex platelet structure. These films were thick, rubbed off easily with a tissue, and were a deep yellow color. The solution from which this sample was removed did not initially have large amounts of $Cd(OH)_2$ precipitate but did, upon careful inspection, show a slight amount of precipitate. At still higher pH values, in solutions with greater amounts of $Cd(OH)_2$ precipitate, similar films morphologies were observed but tended to be thicker yet. The morphology of the sample obtained at a pH of 10.03 (Figure 4b) consisted of a single layer of densely packed spherulites. The film was tightly adhered to the surface and could not be removed by light abrasion with a tissue. These films were specularly reflecting and had a distinct yellow tint. The solution from which this sample was obtained contained no discernible $Cd(OH)_2$ precipitate. As shown in Figure 4c,d, similar morphologies were obtained on samples prepared at lower pH values. The major difference was a decrease in the number density of spherulites with decreasing pH. This trend was continued down to a pH of 7.00, at which point thiourea decomposition was negligibly slow and no films were deposited. The two film morphologies correlated with the presence or absence of a bulk $Cd(OH)_2$ precipitate. Presence of the precipitate led to thick, powdery films of poor quality; while in the absence of $Cd(OH)_2$ uniform, adherent films were formed.

Figure 4b–d shows some variation in spherulite size. The range of sizes shown was typical of batch-to-batch variations and did not appear to vary with pH. As discussed at length below, the crystallite diameter increases linearly with time and the variation observed in Figure 4 may be due in part to the time at which a particular experiment was terminated.

Film elemental composition was determined by XPS. Quantitative analysis of the film composition was performed by correcting the XPS peak intensities by using published values of the scattering cross sections. As the best quality CdS films were formed at pH values below where $Cd(OH)_2$ bulk precipitate was present, XPS was conducted only on these films. XPS results are also presented for samples exposed to solutions to which thiourea was not added. In this manner the effect of solution composition on the substrate could be determined. The samples are multilayered, and the elements were not homogeneously distributed through the samples. The basic substrate was p-doped silicon that supported a silicon dioxide layer approximately 15–20 Å thick. On top of this was the CdS film and, as will become apparent, some $Cd(OH)_2$. In addition, as shown in Figure 4, the CdS films were not uniformly deposited. For these reasons we provide only a semiquantitative discussion of the XPS data and focus on trends in elemental composition with pH.

Typical survey spectra are shown in Figure 5 for films formed with and without the addition of thiourea at pH 9.68. The elements present were oxygen, cadmium, carbon, sulfur, and silicon. Note that cadmium was present even in the absence of thiourea. This suggested the physisorption of cadmium or the presence of a $Cd(OH)_2$ film. In the absence of thiourea, silicon and oxygen still dominate the spectra; in the presence of thiourea, silicon was much reduced and oxygen much diminished relative to cadmium and sulfur. The metallic silicon 2p peak from the substrate and the silicon 2p peak from the oxide layer can be resolved in these spectra. For the samples without thiourea, the silicon dioxide peak was discernible only as a shoulder on the side of the much larger metallic silicon peak. After deposition of a CdS film, the metallic silicon 2p peak was much reduced and become comparable in intensity to the

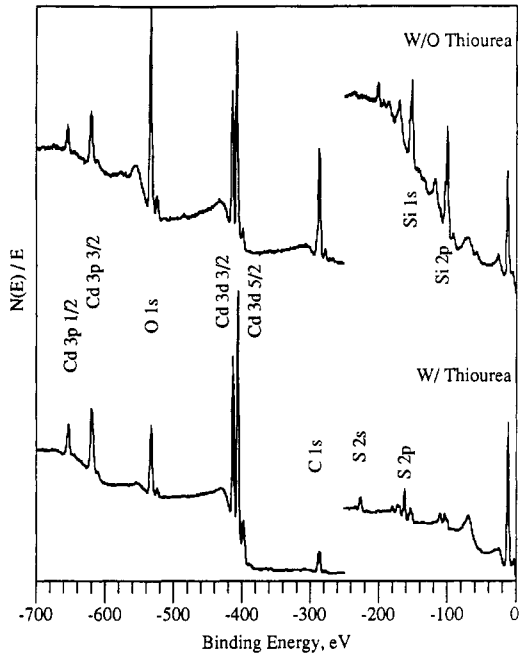

Figure 5. XPS survey spectra of samples at pH 9.68 with (bottom) and without (top) addition of thiourea. The scale for data below −250 eV is expanded 4 times.

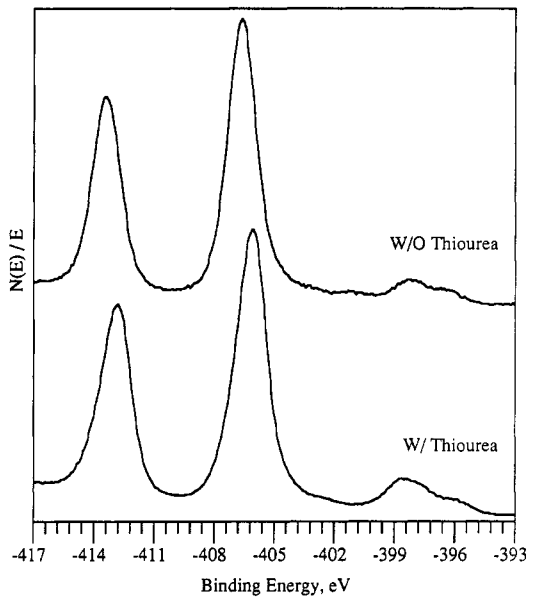

Figure 6. XPS multiplex spectra of samples at pH 9.68 with (bottom) and without (top) addition of thiourea in the region of the cadmium 3d 3/2, cadmium 3d 5/2, and nitrogen 1s peaks.

silicon dioxide 2p peak. Such trends were typical for the entire range of sample pH values examined. A more quantitative examination is given below. The carbon 1s peak was present in these samples but was of little informational utility as carbon is present as an impurity in almost all samples exposed to atmosphere and analyzed by XPS. The carbon peak was used to correct for charging effects.

Nitrogen may be present as $CdCN_2$ but unfortunately the nitrogen 1s line was obscured by the very intense cadmium 3d 5/2 peak. To determine the possible presence of nitrogen as $CdCN_2$, multiplex spectra were taken in the 400-eV binding energy region. These spectra are shown in Figure 6 samples with and without added thiourea at pH 9.86 and hence with and without possible formation of $CdCN_2$. Similar results were observed for other samples.

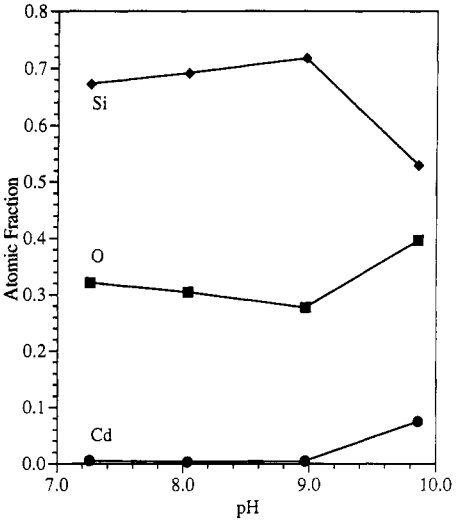

Figure 7. Elemental atomic fractions versus pH in the absence of thiourea for silicon (◆), oxygen (■), and cadmium (●). Data were calculated from XPS spectra.

The spectra were essentially identical, indicating that $CdCN_2$ was not present in the films. As pointed out above, H_2CN_2 and its acid dissociation products do form in solution in significant quantities but apparently were not incorporated in the films.

Shown in Figure 7 are the atomic fractions of oxygen, silicon, and cadmium for samples immersed in solutions at four pH values but in the absence of thiourea. Silicon was the dominant element and because the silicon/oxygen ratio greatly exceeded 0.5, the XPS sampling depth (approximately 50 Å), as expected, extended well past the SiO_2 oxidation layer into the silicon substrate. Silicon exhibited a slight decrease and oxygen a slight increase in intensity at the highest pH, which suggested a slight increase in thickness of the SiO_2 layer. However, while cadmium was just detectable at the lowest pH values, its atomic fraction was 0.08 at the highest pH. Cadmium may either have physisorbed to the substrate or formed a thin cadmium hydroxide layer. The formation of a $Cd(OH)_2$ layer would also result in a decrease in silicon intensity and increase in oxygen intensity. A sampling volume of 50 Å, a silica layer 20 Å thick, and a $Cd(OH)_2$ layer 15 Å thick gives atomic fractions of 0.09 cadmium, 0.37 oxygen, and 0.54 silicon. The experimental values at pH 9.68 were 0.08 cadmium, 0.40 oxygen, and 0.52 silicon.

As shown in Figure 2, in the pH range 7.0–11.0, the cadmium hydroxide species present have charges of +3, +2, +1, and 0. Above pH 11, the negatively charged hydroxide species become the major species. The silicon substrate used in these studies has a native oxide layer approximately 20 Å thick that should, as on bulk silica, assume a negative ζ potential at these pH values. On this basis, it would be reasonable to expect physisorption of positive cadmium hydroxide species to the surface at pH values below 11. However, once the surface charge is neutralized or has become positive, further physiosorption is unlikely. Furthermore, from the equilibrium diagrams of Figures 1 and 2 it is clear that the concentration of free cadmium decreases precipitously with increasing pH over the 7.0–10.0 pH range. It seems unlikely that the amount of free cadmium adsorbing to the substrate increased over the same pH range. The same can also be said for Cd_2OH^{3+} and in part for $CdOH^+$. Thus on the basis of equilibration of one or more of these species with the surface adsorbed

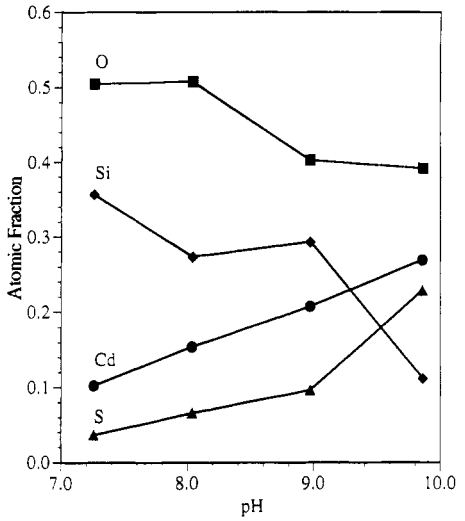

Figure 8. Elemental atomic fractions versus pH in the presence of thiourea for silicon (◆), oxygen (■), cadmium (●), and sulfur (▲). Data were calculated from XPS spectra.

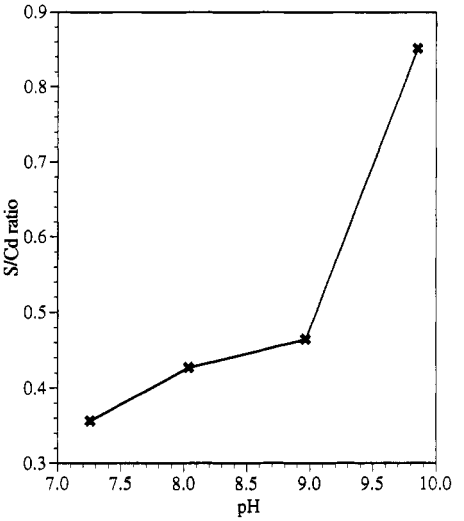

Figure 9. Cadmium/sulfur ratio showing stoichiometry of films. Data derived from Figure 8.

species, one might expect a decrease in physisorbed cadmium as detected in the XPS experiments. Alternatively, at pH 9.86 the solution was just at the point where the species $Cd(OH)_2$ began to increase and just below pH 10.40 where bulk precipitation began to appear. As an uncharged species $Cd(OH)_2$ may form a thin film on the silica substrate which apparently is stable at pH values just below that of bulk $Cd(OH)_2$ precipitate.

In summary, three pH regimes can be identified for $Cd(OH)_2$ formation in the absence of thiourea. Below pH 9, $Cd(OH)_2$ was not found in solution nor in significant amounts on the silicon substrates. Between pH 9 and 10.4, a $Cd(OH)_2$ layer was found on the substrates but not in solution. Above pH 10.4, $Cd(OH)_2$ was found both in solution and on the substrate.

Shown in Figure 8 are the XPS versus pH results for samples in the presence of thiourea. Oxygen was the dominant element. The ratio of silicon to oxygen at low pH indicated that the underlying silicon substrate was still within the XPS sampling depth for this material, although not nearly to the extent seen for samples without thiourea. At high pH the interpretation of the silicon/oxygen ratio was complicated by the presence of cadmium and possible formation of $Cd(OH)_2$. The decreased sampling of the silicon substrate was most certainly due in part to the overlying CdS layer but may also be due to an increase in the thickness of the SiO_2 layer and/or the presence of a $Cd(OH)_2$ layer.

Cadmium showed an increase in atomic fraction from 0.10 at the lowest pH to 0.25 at the highest pH. This increase was consistent with the micrographs of Figure 4 in which the number density of spherulites and hence the amount of cadmium increases with pH. Sulfur shows a similar trend but the films are distinctly substoichiometric. Plotted in Figure 9 is the atomic ratio of sulfur to cadmium taken from Figure 8. At the lowest pH, the film is 36% CdS and 64% $Cd(OH)_2$. At the highest pH, the film is 86% CdS and 14% $Cd(OH)_2$. Clearly, increased pH resulted in more stoichiometric CdS films. At low pH, the absence of a significant $Cd(OH)_2$ layer in the absence of thiourea indicated that hydroxide was being incorporated into the cadmium sulfide films during deposition and was not deposited as a separate layer. At pH 9.68, the presence of a thin film of $Cd(OH)_2$ was suspected and the CdS may be deposited on top of this layer. In this case, the stoichiometry of the CdS layer may be better than the data indicated.

To follow the kinetics of film growth, samples were removed from a solution at pH 9.55 at various times up to 4000 min. The films were examined by electron microscopy to obtain the number density and diameter of the spherulites. The film from a portion of each sample of known area was dissolved in 10% nitric acid and the cadmium content determined by atomic absorption. Shown in Figure 10 are selected electron micrographs of the CdS films. At 960 min, Figure 10a, no particles were present on the surface. At longer times, Figure 10b–d, a distinct increase in particle size was observed and at least qualitatively the number of particles per unit area was approximately constant. A quantitative analysis of these quantities is shown in Figure 11. Shown are the nanomoles of cadmium per square centimeter area, Figure 11a, as determined by atomic absorption; the number of nuclei per square micrometer, Figure 11b, and the nuclei diameter in micrometers, Figure 11c, as measured from the micrographs.

The amount of cadmium per unit area shows an approximately exponential or power law increase with time and suggests that an autocatalytic process was involved which enhanced the rate with progression of the reaction. After 3500 min, bulk precipitate began to appear and resulted in many adhered particles. This effectively terminated the experiment by removing thiourea and cadmium from solution. Atomic adsorption results after 3500 min exhibited an order of magnitude jump in cadmium content because of adhered particles and were not considered valid for rate analysis. The number of nuclei were determined by counting the number of crystallites and assuming a one-to-one correlation between nucleation events and number of crystals. Below 1400 min no crystallites could be discerned at 80 000× magnification, and the substrates appeared identical to bare silicon. A distinct jump in the number of nuclei was observed at 1400 min from zero to an essentially constant average value of 63 nuclei/μm^2. The nuclei diameter, Figure 11c, showed a steady increase in size with time once nucleation was initiated. It can be observed qualitatively from the micrographs that the particle size distribution was narrow at early times and that particle

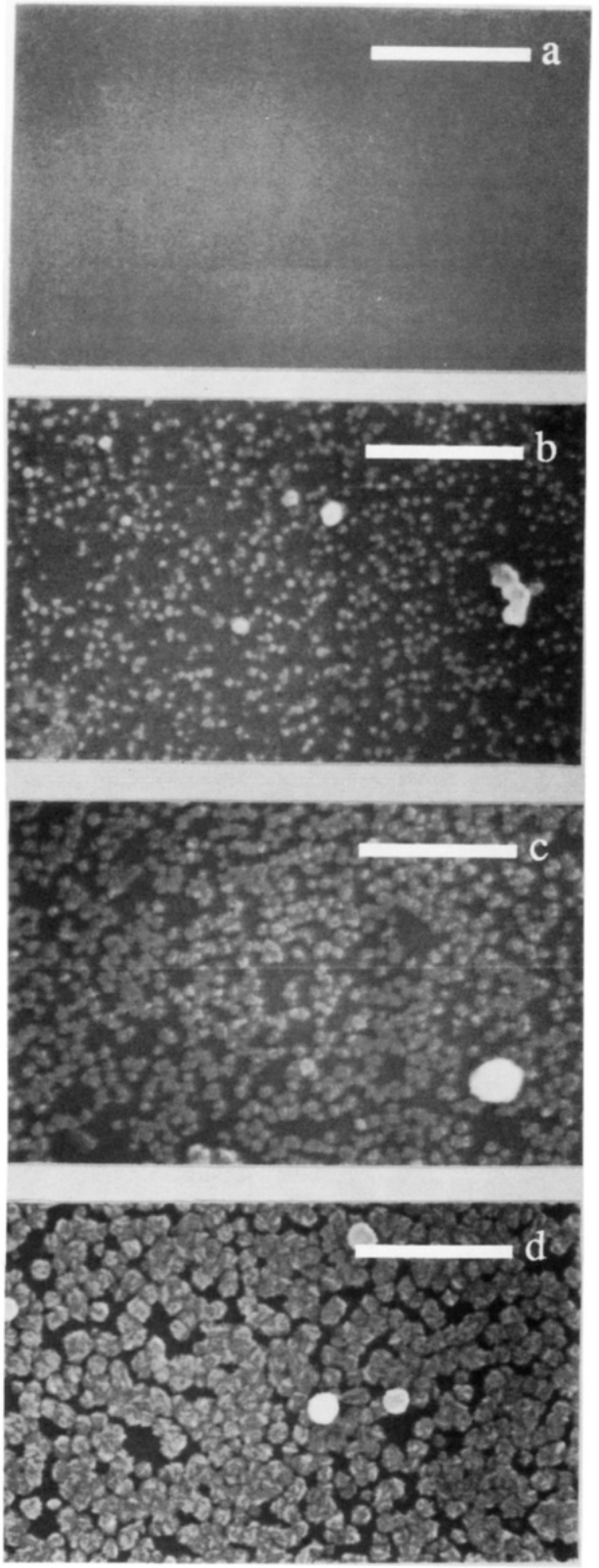

Figure 10. Scanning electron micrographs of CdS films from samples removed at various times. Solution pH was 9.55. Times are 960 (a), 1920 (b), 2880 (c), and 3840 min (d). The scale bars represent 1 μm.

growth did not noticeably lead to widening of the distribution at longer times.

These results were similar in behavior to burst type nucleation observed in homogeneous precipitation in bulk

(26) Mutijevic, E. *Langmuir* **1986**, *2*, 12.

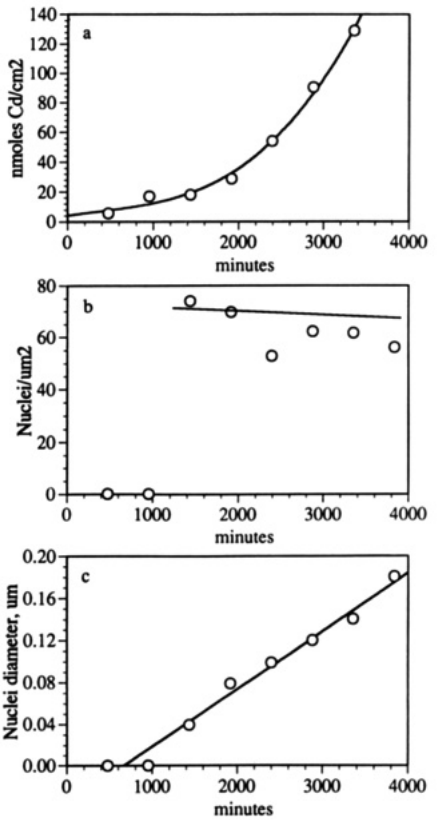

Figure 11. Film growth data for CdS films versus time at pH 9.55. Nanomoles/cm^2 of cadmium deposited as determined by atomic absorption analysis (a), number of nuclei/cm^2 from electron micrographs (b), and average nucleus diameter in microns from electron micrographs (c).

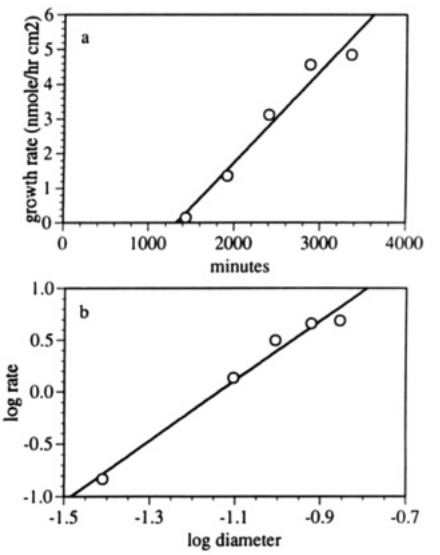

Figure 12. Analysis of film growth data. Cadmium deposition rates (nmol of Cd/h) versus time using the data from Figure 11a (a) and logarithm of the rate of cadmium deposition versus logarithm of the nuclei diameter taken from Figure 11c (b).

solution.[26] In this type of precipitation, the precipitating reagent is generated in situ, by reactions such as the solution decompositioon of thiourea, and avoids the localized concentration gradients associated with volumetric addition of the precipitating reagent. An induction period is observed as the degree of supersaturation increases uniformly throughout the solution. A sudden burst of nuclei are formed in solution once the supersaturation surpasses that required for spontaneous homogenous nucleation. The burst consumes reagent and

decreases the supersaturation such that homogenous nucleation is no longer possible. Crystal growth commences and the growth rate is determined by the rate of precipitating reagent generation. Because the nuclei are formed at a single point in time and the conditions for growth are uniform with time, a very narrow size distribution of crystallites is obtained. A very similar interpretation can be applied to the data of Figure 11 except that nucleation and growth occurred on a surface and not in bulk. In this case formation of a bulk precipitate did not occur until times greater than 3500 min and we cannot attribute film formation to adherence of bulk formed nuclei.

While the electron micrographs exhibited no trace of nuclei at early times, the atomic absorption data clearly showed the presence of cadmium. To gain some perspective on cadmium coverage, the first atomic adsorption data point at 460 min has a cadmium content of 5.4×10^{-9} mol/cm^2. Using a density of 4.79 g/cm^3 for $Cd(OH)_2$, the layer was calculated to be 17 Å thick, in very good agreement with the XPS data.

At times above 1000 min the amount of cadmium deposition increased approximately exponentially with time. Shown in Figure 12a is the growth rate as a function of time. The rate clearly increased with time over the period shown in figure. Eventually, of course, the rate decreased as the solution was depleted of reagents. But this did not happen until substantial amounts of bulk precipitation occurred, and reliable data could not be obtained at these long times because bulk particulates adhered to the surface. Over the 3500 min of this experiment, with slow growth rates and in stirred solutions, mass transfer is unlikely to be the limiting step. In addition depletion of the solution reagents would be exhibited as a decrease in rate with time. Over the times relevant to Figure 12a, the amount of CdS deposited was very small and the concentration of cadmium and thiourea remained essentially constant and equal to the initial values. Thus, the rate of generation of sulfide by homogeneous decomposition of thiourea should have been constant during these early times. From this we can conclude, at best, that the rate of growth if limited by reagent concentration should have been constant with time and not have increased with time.

An increase in growth rate can be explained by some autocatalytic process or by a process dependent on surface area. In Avrami crystal growth kinetics[27] the time rate of change of the crystal volume for instantaneously formed nuclei is dependent only on the crystal geometry. For hemispherical growth symmetry, the crystal volume change is given by

$$dV/dt = {}^1/_2 A\, dD/dt$$

where D is the diameter, dD/dt is the growth velocity, and A the surface area of a sphere of diameter D. An alternative expression in terms of mass of CdS deposited is

$$d[CdS]/dt = \rho/(MW/2)A\, dD/dt$$

The Avrami derivation contains no mechanistic assumptions except in the growth velocity term. This term may be determined by mass transfer, ion absorption, surface diffusion, or site incorporation steps. It may also be determined by heterogeneous decomposition of the reagents and in this case decomposition of thiourea. It may be presumed that this rate is dependent on the surface area of the particles upon which thiourea may be adsorbed. In this case the inorganic substrate was CdS and growth of the particles resulted in enhanced thiourea decomposition. The rate can then be written

$$d[CdS]/dt = k[Cd^{2+}][TU]A$$

where k is the absolute rate constant, [TU] is the concentration of thiourea, and A is the area available for thiourea decomposition. As reagent concentration is constant of over the time frame of this experiment, the rate relationship is more simply written as

$$d[CdS]/dt = k'A$$

This expression is similar to the basic Avrami equation if growth velocity is constant over time. Figure 11c plots the nuclei diameter versus time. The slope of this plot is the growth velocity and is easily fitted with a linear line of constant slope. Thus the Avrami equation reduces to the equation derived assuming a thiourea decomposition mechanism.

The data from Figure 11a plots [CdS] in units of nmol/cm^2 as a function of time and the term $d[CdS]dt$ can be obtained from these data. This analysis is plotted in Figure 12a. On the basis of the electron micrographs, the particles can be taken as hemispheres with a nominal area proportional to D^2. However, the surface of the particles was clearly convoluted and the actual surface area depends upon the precise topography of the surface. If the surface is fractal, then the area is proportional to D^n where $2 \leq n \leq 3$ depending on the type fractal geometry.[28] Substituting this for the area, the equation becomes

$$d[CdS]/dt = k'D^n$$

Taking the log of both sides gives

$$\log (d[CdS]/dt) = \log k' + n \log D$$

The rate was taken from the data for Figure 12a and plotted against the nuclei diameter taken from the data of Figure 11c. This plot is shown in Figure 12b. A line fitted to the data is plotted in the figure and is given by

$$\log (d[CdS]/dt) = 3.3 + 2.8 \log D$$

to give a value for n of 2.8. The value of n is between 2.0 and 3.0 as is required by fractal theory for dimensionality of the surface area.

The data presented in Figures 11 and 12 are consistent with a thiourea decomposition mechanism but do not exclude other mechanisms which may also have linear growth rates. The literature contains a number of reports[16-18] concluding that metal hydroxide and metal sulfide particles catalyze the decomposition of thiourea. In particular, Norr[17] found PbS to catalyze thiourea decomposition. From this it is plausible that CdS also is catalytically active and our analysis of the rate data support this conclusion.

Conclusions

The morphology and kinetics of film formation are controlled by the presence or absence of a $Cd(OH)_2$

(27) Tiller, W. A. *The Science of Crystallization: Microscopic Interfacial Phenomena*; Cambridge University Press: Cambridge, 1991, p 376.

(28) Feder, J. *Fractals*; Plenum: New York, 1988.

precipitate in solution or a $Cd(OH)_2$ film on the substrate surface. Three distinct regions were identified. At pH less than 9.0, no precipitate or substrate film was detected. Spherulitic crystals formed in this region but were sparsely distributed. From pH 9.0 to 10.4, a $Cd(OH)_2$ film was found on the surface. Adherent, specularly reflecting, densely packed uniform films were formed under these conditions. Above pH 10.4, a $Cd(OH)_2$ precipitate was formed in solution. Poor-quality thick CdS films were formed. Decomposition of thiourea was very rapid and was complete in less than 2 h.

The presence of the $Cd(OH)_2$ film correlated well with the formation of the best quality film. In light of the ability of $Cd(OH)_2$ to catalyze thiourea decomposition in bulk, this film may act in a similar manner to localize decomposition at the surface and promote film formation rather than bulk precipitate formation. Spherulitic films, of considerably more sparse coverage, were also formed at pH values where $Cd(OH)_2$ was not present. This may indicate that the silica surface also catalyzes thiourea decomposition but to less extent than the $Cd(OH)_2$ surface.

The kinetics of film growth were measured under conditions where a $Cd(OH)_2$ film was formed but no precipitate was found in solution. By analyzing the mass deposited, the number of nuclei formed, and the growth with time, the kinetics were shown to be similar to burst type nucleation and crystal growth in solution except that in this instance nucleation and growth were confined to the surface. This leads to films of high density, good uniformity, and monodispersed crystallite size. The rate of film growth was found to increase with time and be proportional to surface area if the particles were assumed to have a fractal area. Surface-catalyzed decomposition of thiourea by CdS particles was an appropriate explanation.

The speciation calculations identified the important species involved in film formation. Most of the cadmium was complexed as the $Cd(NH_3)_x^{2+}$ species above pH 7.0. Contrary to previous reports,[6,7] amine-complexed cadmium was present under all important deposition conditions and did not correlate with changes in deposition rates for film morphology. The role of the amine complexant was to control the amount of free cadmium in solution and consequently control the pH at which the various $Cd_x(OH)_y^{2x-y+}$ species became dominant.

For deposition of high-quality, adherent, phase-pure CdS films it appears that a surface catalytically active toward thiourea decomposition is desirable. In this work a $Cd(OH)_2$ film was responsible for this effect. In considering deposition on other substrates, this film may or may not form under suitable conditions. Some control over its formation may be accomplished by controlling the concentration of amine complexant; although we have not fully explored this approach. Alternatively, many substrates may be inherently catalytic toward thiourea decomposition or it may be possible to chemically modify the surface to make it actively catalytic.

Acknowledgment. The authors thank Mark Englehard (XPS), Jim Coleman (SEM), and Penny Colton (Atomic Absorption) for their analytical analyses. We are indebted to Bruce Bunker and Paul Calvert for their critical readings of the preliminary manuscripts. This research was supported by the U.S. Department of Energy, Office of Basic Energy Sciences under Contract DE-AC06-76RLO 1830. Pacific Northwest Laboratory is operated for the U.S. Department of Energy by Battelle Memorial Institute.

Registry No. CdS, 1306-23-6; $Cd(OH)_2$, 21041-95-2; thiourea, 62-56-6.